ARTICLE

Improving Interfacial Electrochemistry of $LiNi_{0.5}Mn_{1.5}O_4$ Cathode Coated by Mn_3O_4

Miao-miao Deng[a,b], Da-wei Zhang[a], Yu Shao[b], Xiao-dong He[b], Aqsa Yasmin[b], Chun-hua Chen[b*]

a. School of Chemistry and Chemical Engineering, Heifei University of Technology, Hefei 230009, China

b. Chinese Academy of Science Key Laboratory of Materials for Energy Conversions, Department of Materials Science and Engineering & Collaborative Innovation Center of Suzhou Nano Science and Technology, University of Science and Technology of China, Hefei 230026, China

(Dated: Received on June 12, 2019; Accepted on August 14, 2019)

In this work the surface of $LiNi_{0.5}Mn_{1.5}O_4$ (LMN) particles is modified by Mn_3O_4 coating through a simple wet grinding method, the electronic conductivity is significantly improved from 1.53×10^{-7} S/cm to 3.15×10^{-5} S/cm after 2.6 wt% Mn_3O_4 coating. The electrochemical test results indicate that Mn_3O_4 coating dramatically enhances both rate performance and cycling capability (at 55 °C) of LNM. Among the samples, 2.6 wt% Mn_3O_4-coated LNM not only exhibits excellent rate capability (a large capacity of 108 mAh/g at 10 C rate) but also shows 78% capacity retention at 55 °C and 1 C rate after 100 cycles.

Key words: Lithium-ion batteries, Cathode materials, Spinel lithium nickel manganese oxide, Surface modification, Cathode-electrolyte interphase

I. INTRODUCTION

Spinel-type $LiNi_{0.5}Mn_{1.5}O_4$ (LNM) exhibits a theoretical capacity of 147 mAh/g and a competitive energy density of 640 Wh/kg at a higher working voltage (∼5 V) [1–3]. Nevertheless, the practical use of a LNM cathode is restricted by its poor high-rate capability and dramatic capacity decay at high temperature, which mainly result from the side reaction that occurs on the cathode-electrolyte interphase. An effective strategy of surface coating has been introduced to strengthen the stability of the cathode-electrolyte interphase and eliminate the side reaction. The reported surface coating materials, including Al_2O_3 [4], CuO [5], ZnO [6], RuO_2 [1], TiO_2 [7], carbon [8, 9], Li_3PO_4 [10] and $Li_4Ti_5O_{12}$ [11] have been proven to boost the electrochemical property of LNM. However, the rate performance especially at a large current density (10 C), of LNM modified with the reported coating materials (except carbon materials) is unsatisfactory. With respect to the carbon materials, the redox reaction between carbon and Mn^{4+} cannot be neglected during high temperature treatment. Therefore, discovering for a new coating material LNM is necessary and urgent.

According to the literature reports [12–14], electrochemically inactive Mn^{4+} existing on the surface of cathode particles can provide excellent structural stability during electrochemical cycling. Additionally, our previous work [15] reported that the right amount of Mn^{3+} on the surface of LNM particles is beneficial to improve the electrical conductivity of LNM. Hence, we deposit a Mn_3O_4 coating layer on the surface of LNM particles, which can combine the electrochemical inactivity of Mn^{4+} and active Mn^{3+} ions. Moreover, the Mn_3O_4 coating matches well with LNM due to their same spinel-type crystal structure, which is favorable for Li^+ diffusion at the interface. Undoubtedly, the results of electrochemical measurements demonstrate the significant rate performance and cycling stability (at 55 °C) after Mn_3O_4 coating. Therefore, this work provides a different direction of thinking while selecting the materials for the surface modification of LNM material, which is not only limited to the common inert materials, but will be extended to some electrochemical active materials in the future research.

II. EXPERIMENTS

The LNM sample was obtained via a thermopolymerisation method reported in the previous work [15]. Lithium nitrate ($LiNO_3$, 5% excess), nickel nitrate ($Ni(NO_3)_2{\cdot}6H_2O$), and manganese acetate ($Mn(CH_3COO)_2{\cdot}4H_2O$) were together dissolved in distilled water. Then, acrylic acid (AA) was added to form a mixed solution with volume ratio of 1:2, and then placed in an oven at 150 °C for 10 h to obtain a fluffy powder product. The powder was first calcined at 500 °C for 5 h and then ground into a fine powder to obtain an intermediate product, which was sintered at 900 °C for 15 h and subsequently annealed at 700 °C for

Author to whom correspondence should be addressed. E-mail: cchchen@ustc.edu.cn

48 h. All these heat treatment processes were carried out in air atmosphere.

For the preparation of Mn_3O_4-coated LNM samples, different amounts of manganese acetate ($Mn(CH_3COO)_2{\cdot}4H_2O$) were dissolved in ethanol in mortar, and then mixed with the as-prepared LNM powder to obtain the intermediate powders. Finally, the calcining process was performed at 400 °C in air for 5 h to obtain the final X wt% Mn_3O_4-coated LNM (X=0.9, 2.6, 4.4) samples.

To understand the state of Mn_3O_4 coating, we also followed the same procedure to treat manganese acetate alone at 400 °C for 5 h. As evident in FIG. S1 in supplementary materials, in comparison with Mn_3O_4 (PDF#24-0734), the product was indeed Mn_3O_4.

A scanning electron microscope (SEM, JSM-6390LA), transmission electron microscope (TEM, JEM-2100F), and X-ray diffraction (XRD) measurement at a scanning rate of 10 °/min were introduced to analyse the structure and morphologies of particles. The oxidation state change of the Mn ions was checked by X-ray photoelectron spectroscopy (XPS, ESCALAB 250). The Fourier transformed infrared (FTIR) tests were studied with a Nicolet 8700 infrared spectrometer.

Electrochemical impedance spectroscopy (EIS) was performed at an electrochemical workstation (CHI 604A) over the frequency range from 0.01 Hz to 10^5 Hz. The prepared cells for the EIS measurements must be cycled at 0.2 C for 3 times and then charged to half of the capacity. Cyclic voltammetry (CV) was performed using the same electrochemical workstation at a scan rate of 0.1 mV/s.

The positive electrodes were prepared as follows: the prepared homogenous slurries, fabricated with 8:1:1 mass ratio of active materials (*i.e.* LNM and Mn_3O_4@LNM), acetylene black, and PVDF in N-methyl-2-pyrrolidone, were casted onto an aluminum foil and dried at 70 °C overnight in a vacuum oven. The loading content of the electrode materials is around 3.3 mg/cm^2. The electrodes were tested by CR2032 cells assembled in an Ar-glove box. Next, 1 mol/L $LiPF_6$ was mixed in ethylene carbonate—dimethyl carbonate (1:1, w/w) to prepare the electrolyte. The cells were measured on a Neware BTS2300 battery cycler within a voltage range of 3.5−4.9 V at room temperature (25 °C).

To measure the electrical conductivity of LNM and the Mn_3O_4-coated LNM powders, firstly, the powders were respectively pressed into discs (diameter in 14 mm), and then coated with silver paste on both sides of the discs.

III. RESULTS AND DISCUSSION

A. Crystal structures and particle morphology

The XRD patterns for all the samples are presented in FIG. 1(a). Impurities such as $Li_xNi_{1-y}O$ with diffraction peaks located at 2θ =37.5°, 43.6° and 63.4° can be hardly detected in the XRD patterns [15, 16]. Besides, the sharp and intensive diffraction peaks can be well indexed as cubic spinel-structured LNM. Nevertheless, no diffraction peaks of Mn_3O_4 or other manganese oxides are detected in the XRD patterns. In comparison with Mn_3O_4 (PDF#24-0734), we find that the characteristic diffraction peaks of Mn_3O_4 overlap with that of LNM.

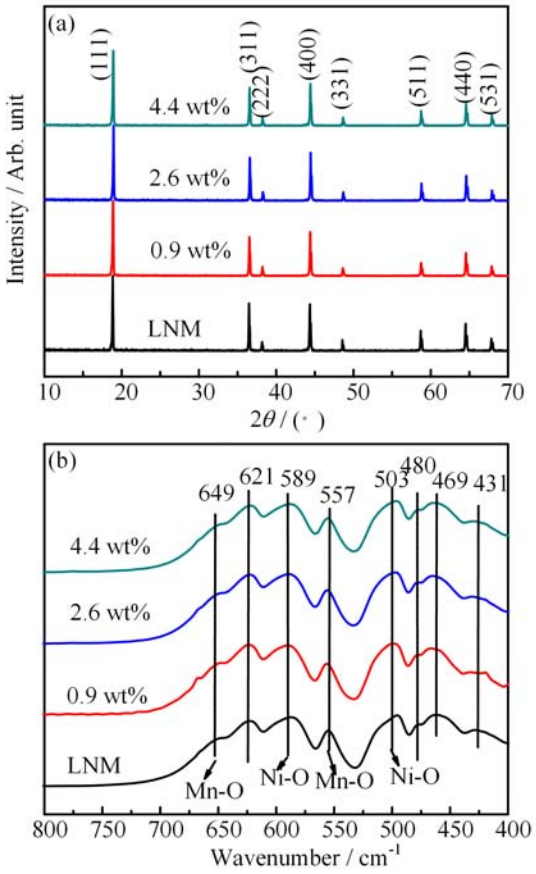

FIG. 1 (a) XRD patterns and (b) FTIR spectra of the samples: 0 wt%, 0.9 wt%, 2.6 wt%, 4.4 wt% Mn_3O_4-coated LNM.

The space group of LNM is verified by the FTIR measurement shown in FIG. 1(b). Generally, eight IR adsorption peaks could be detected for LNM with a $P4_332$ structure in the FTIR spectra while only five could be detected for their disordered counterparts (Fd3m) [17, 18]. In FIG. 1(b), the Mn_3O_4-coated LNM samples display eight intensive adsorption peaks that are the same as those observed for pristine LNM, which proves that the coating modification process maintains the $P4_332$ space group.

The SEM images of the pristine and coated samples are shown in FIG. 2. The pristine LNM samples are octahedron-shaped particles with an average size of 2 μm, and their surfaces are smooth and clean (FIG. 2(a)). Meanwhile, the Mn_3O_4-coated samples display much rougher surfaces (FIG. 2(b−d)).

DOI:10.1063/1674-0068/cjcp1906118

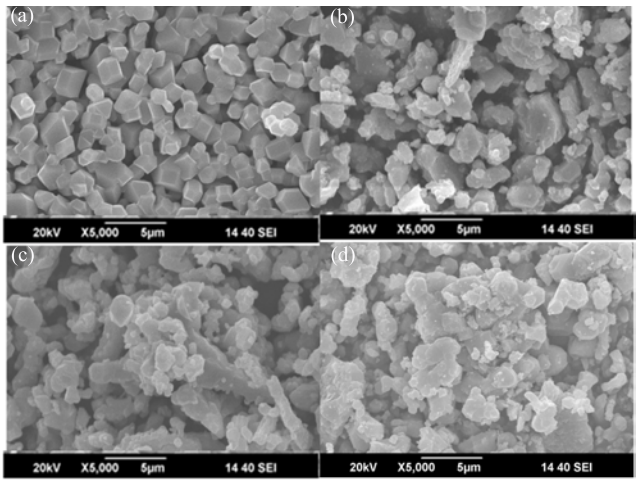

FIG. 2 SEM images of (a) 0 wt%, (b) 0.9 wt%, (c) 2.6 wt%, and (d) 4.4 wt% Mn_3O_4-coated LNM.

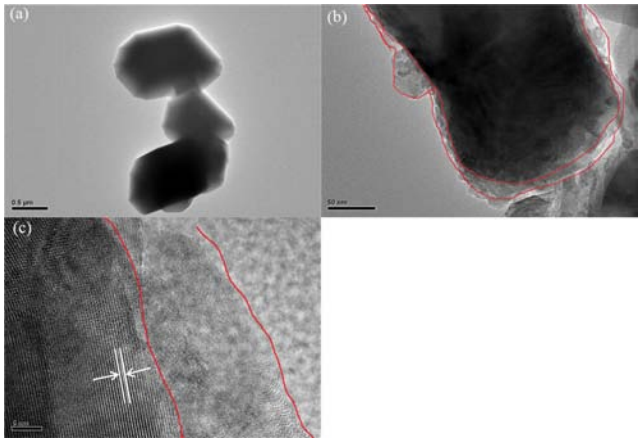

FIG. 3 TEM images of (a) LNM, and (b) 2.6 wt% Mn_3O_4-coated LNM, (c) HRTEM image of 2.6 wt% Mn_3O_4-coated LNM.

As a representative, the coating layer of 2.6 wt% Mn_3O_4-coated LNM is observed by HRTEM, the results are shown in FIG. 3 (b) and (c). The surface of the pristine sample is smooth in FIG. 1(a), while the surface of the coated sample is covered by a coating layer of an average thickness of 20 nm. In the HRTEM image (FIG. 3(c)), only a few of lattice fringes can be detected for the Mn_3O_4 coating layer, which indicates its poor crystallization degree.

In addition, the valence states of Mn in these samples were analysed by XPS. FIG. 4 (a−c) show the XPS spectra of Mn 2p region, in which the peaks at 643.0 and 655.0 eV are assigned to Mn $2p_{3/2}$ and Mn $2p_{1/2}$. For the major peaks of Mn $2p_{3/2}$, the peaks at 642.4 and 643.3 eV are attributed to Mn^{3+} and Mn^{4+} [1, 9, 19, 20], respectively. The content of Mn^{3+} was estimated based on the peak area ratio of $Mn^{3+}/(Mn^{3+}+Mn^{4+})$ in Mn $2p_{3/2}$ (FIG. 4(d)). Thus, the $Mn^{3+}/(Mn^{3+}+Mn^{4+})$ ratio of 0 wt%, 2.6 wt%, and 4.4 wt% Mn_3O_4-coated LNM samples were calculated to be 33.45%, 45.54%, and

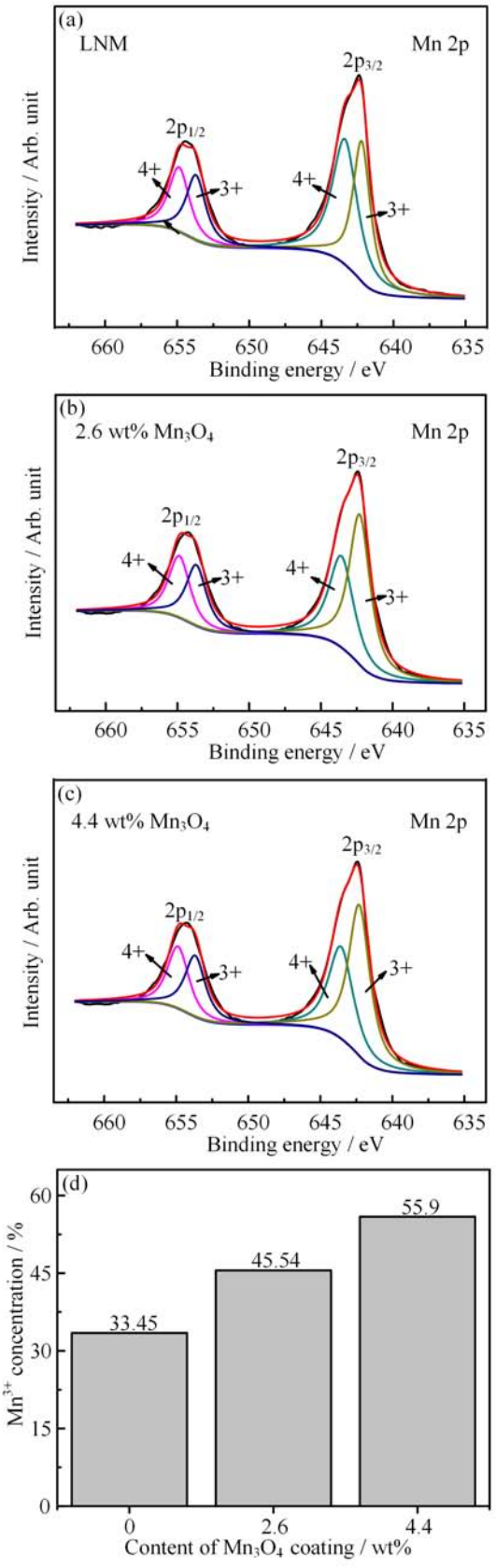

FIG. 4 XPS spectra of samples: Mn 2p for (a) 0 wt%, (b) 2.6 wt%, and (c) 4.4 wt% Mn_3O_4-coated LNM. (d) Concentration of Mn^{3+} ions calculated by the peak of $2p_{3/2}$.

DOI:10.1063/1674-0068/cjcp1906118

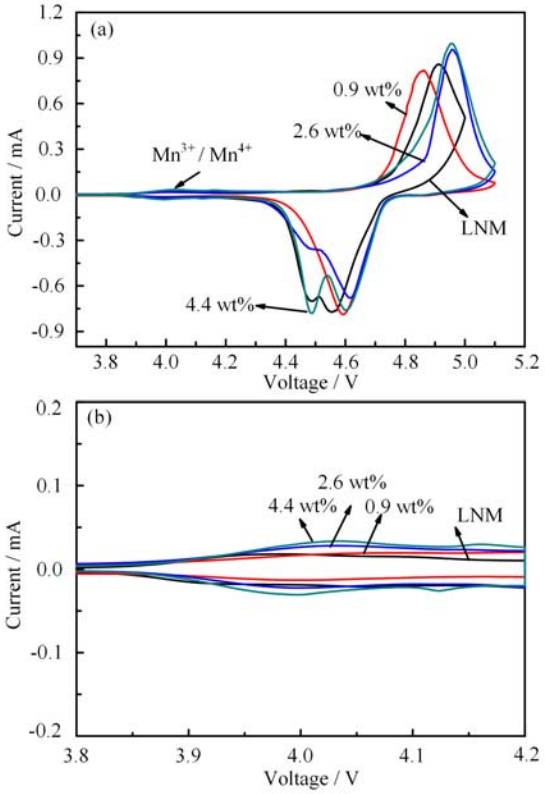

FIG. 5 CV plots of (a) pristine and Mn_3O_4-coated LNM, (b) an enlarged CV curves in the range of 3.8−4.2 V.

55.9%, respectively, which indicates that the amount of Mn^{3+} ions on the surface of samples increases obviously after coating with Mn_3O_4. This further proves that the coating layer is Mn_3O_4.

FIG. 5(a) shows the cyclic voltammograms (CV) of 0 wt%, 0.9 wt%, 2.6 wt%, and 4.4 wt% Mn_3O_4-coated LNM samples. The small peaks at 4.0 V are ascribed to Mn^{3+}/Mn^{4+} redox couples, while the strong peak at approximately 4.7 V to Ni^{2+}/Ni^{4+} redox couples; both can be detected for all samples [1, 3, 19]. From the enlarged CV curves in FIG. 5(b), it can be clearly observed that the content of Mn^{3+} ion increases with the coating content of Mn_3O_4, which is consistent with the XPS results.

B. Electrochemical performance at room temperature

FIG. 6(a) shows the initial charge−discharge curves of the samples. A long voltage plateau at 4.7 V and a short voltage plateau at 4.0 V are observed for Ni^{2+}/Ni^{4+} and Mn^{3+}/Mn^{4+} redox couple, respectively [1, 3] in FIG. 6(a). Furthermore, the plateau at 4.0 V can only be detected for the Mn_3O_4-coated LNM samples. For the 4.4 wt% Mn_3O_4-coated LNM sample, the initial discharge capacity was 128 mAh/g, which is close to that of pristine LNM sample. A slight increase in

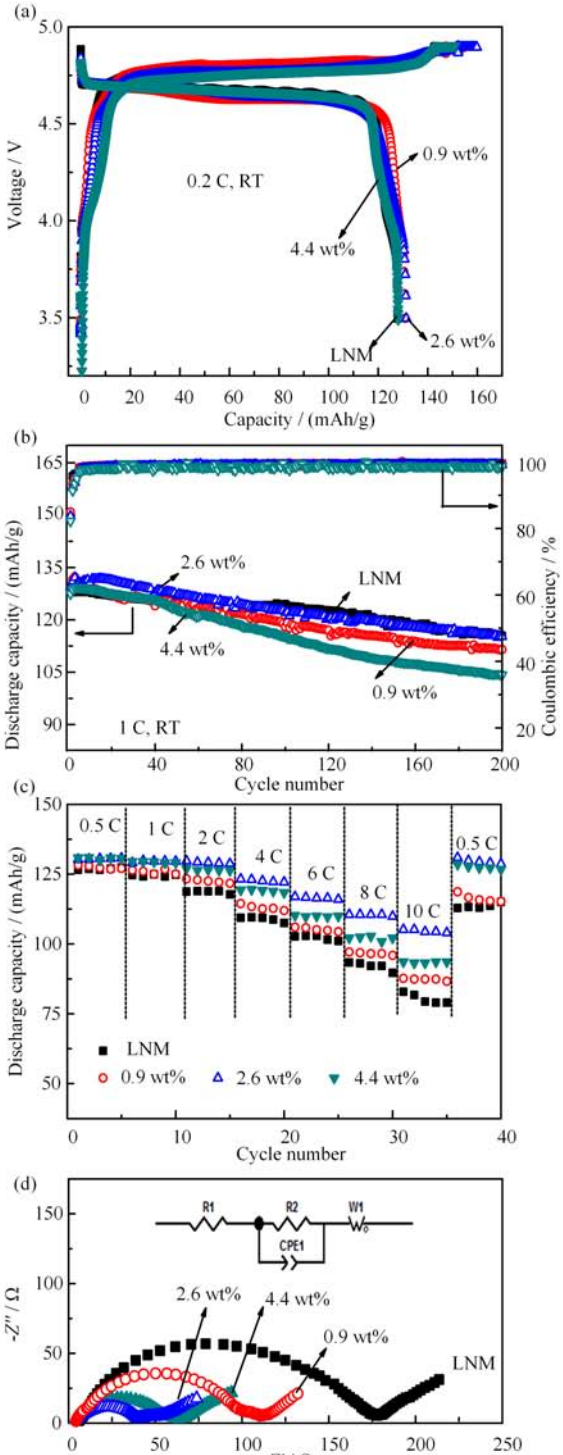

(e)

Sample	R_1 (Ω)	R_2 (Ω)
LNM	6.59	161
0.9 wt% Mn_3O_4	1.55	125.3
2.6 wt% Mn_3O_4	2.83	36.2
4.4 wt% Mn_3O_4	2.53	53.3

FIG. 6 (a) The initial charge-discharge curves at 0.2 C, (b) cycling performance at 1 C, (c) rate performance, (d) EIS spectra of 0 wt%, 0.9 wt%, 2.6 wt% and 4.4 wt% Mn_3O_4-coated LNM at RT and (e) the EIS impedance fitting results of samples.

DOI:10.1063/1674-0068/cjcp1906118

the discharge capacity (about 2 mAh/g) was observed for 0.9 wt% and 2.6 wt% Mn_3O_4-coated LNM samples, which indicates that the lithium ion diffusion between the surface of LNM particles and the electrolyte is not hindered by the Mn_3O_4 coating layer. As shown in FIG. 6(b), the cycling stability and coulomb efficiency of LNM are not enhanced by the addition Mn_3O_4 coating layer.

Then, we tested the rate performance at different current densities, as shown in FIG. 6(c). The rate performance of LNM samples were significantly improved with a Mn_3O_4 coating layer. Further, it should be noted that 2.6 wt% Mn_3O_4-coated LNM sample delivers a discharge capacity of 108 mAh/g at 10 C rate, which is considerably higher than that of pristine LNM (80 mAh/g).

Electrochemical impedance spectroscopy (EIS) was also used to confirm the improved electronic conductivity of Mn_3O_4-coated LNM. The Nyquist plots of these samples are shown in FIG. 6(d). The equivalent circuits and fitting results of the EIS are shown in insets of FIG. 6(d), where R_1 is the ohmic resistance and R_2 is the charge-transfer resistance. Clearly, R_2 decreases from 161 Ω (for LNM) to 36.2 Ω (for 2.6 wt% Mn_3O_4-coated LNM), which suggests the enhanced electronic conductivity of Mn_3O_4-coated LNM. We performed EIS measurements on the sintered pellets of the above two samples (FIG. S2), and the electrical conductivity was calculated using the EIS fitting results. The electrical conductivity of 2.6 wt% Mn_3O_4-coated LNM (3.15×10^{-5} S/cm) was considerably higher than that of pristine LNM (1.53×10^{-7} S/cm). Therefore, the enhanced rate performance of the 2.6 wt% Mn_3O_4-coated LNM is attributed to the high electrical conductivity.

The lithium ion diffusion coefficient is another key factor that determines the rate performance of the electrode materials. The cyclic voltammetry tests for the pristine and 2.6 wt% Mn_3O_4-coated LNM at different scanning rates are shown in FIG. 7. The diffusion coefficient can be calculated by using the Randlnes-Sevick equation [21, 22]

$$i_p = (2.69 \times 10^5) n^{3/2} C_{Li} A v^{1/2} {D_{Li}}^{1/2}$$

where i_p is the peak current (mA), n is the number of electrons per molecule participating in the reaction, D_{Li} is just the diffusion coefficient (cm^2/s), v is the scanning rate (V/s), A is the electrode area (cm^{-2}), and C_{Li} is the concentration of the lithium ion in the electrode (mol/cm^3). For the LNM sample, the C_{Li} value was 0.0243 mol/cm^3 and the electrode area was 1.13 cm^{-2}. Finally, the charge and discharge lithium ion diffusion coefficient of the pristine is 4.57×10^{-10} cm^2/s and 3.33×10^{-10} cm^2/s, respectively. For the 2.6 wt% Mn_3O_4-coated LNM samples, the values were 1.69×10^{-10} cm^2/s and 2.83×10^{-10} cm^2/s, respectively. Based on the above results, the lithium ion diffusion coefficient of these two samples are of the same order of magnitudes, and the difference in the value of the previous digits is small. Therefore, we conclude that the 2.6 wt% Mn_3O_4 coating layer has no effect on the lithium ion diffusion, and its excellent rate performance is attributed to the high electrical conductivity.

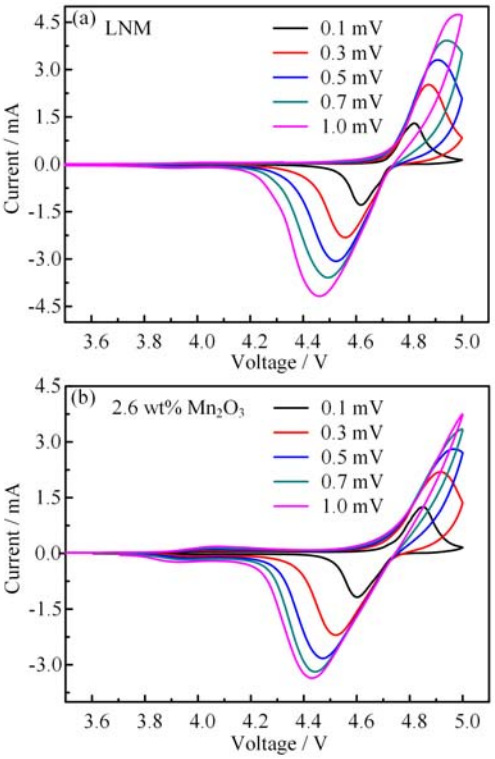

FIG. 7 Cyclic voltammograms of (a) pristine and (b) 2.6 wt% Mn_3O_4-coated LNM at different scanning rates.

C. Cyclic behaviour of the pristine and 2.6 wt% Mn_3O_4-coated LNM at 55 °C

FIG. 8 shows the cycling performances and EIS spectra of the pristine and 2.6 wt% Mn_3O_4-coated LNM samples at 55 °C. For the pristine sample, after 100 cycles, the capacity decreased to 84.6 mAh/g with only 67% capacity retention. However, 2.6 wt% Mn_3O_4-coated LNM exhibited improved cycling stability. Its capacity retention still remains 78%. Moreover, as shown in FIG. 8(b), the 2.6 wt% Mn_3O_4-coated LNM has a lower increase in the impedance compared with the LNM/Li cell; this may be attributed to the Mn_3O_4 coating layer. In fact, at the elevated temperature, the Mn_3O_4 coating layer can reduce the side reactions to some extent, which can be demonstrated from the improved coulomb efficiency in FIG. 8(a). Hence, Mn_3O_4 coating is favorable for improving the cycling stability of LNM at elevated temperatures.

The electrochemical performance of our optimal sample LNM/2.6 wt% Mn_3O_4 was also compared with those

DOI:10.1063/1674-0068/cjcp1906118

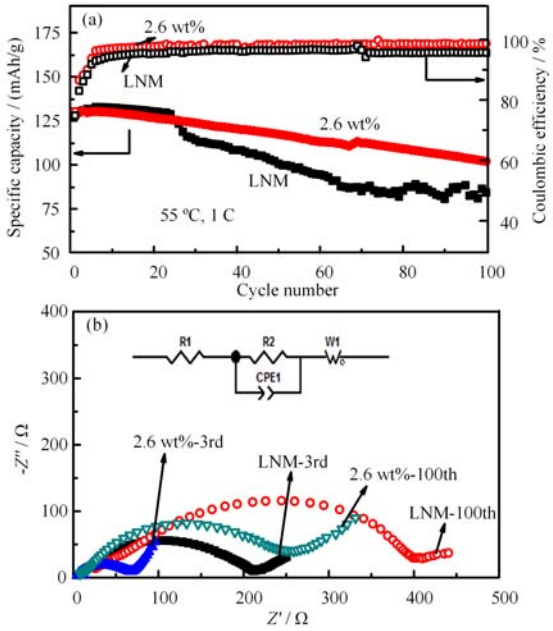

FIG. 8 (a) Cycling performance of the pristine and 2.6 wt% Mn_3O_4-coated LNM at 55 °C and 1 C rate. (b) EIS spectra of these two samples after 3rd and 100th cycles at 55 °C.

of previous reports (Table S1 in supplementary materials), it had one of the best of its rate capability and cycling stability.

IV. CONCLUSION

In this study, we demonstrate that the electrochemical performance of LNM can be significantly improved by the Mn_3O_4 coating layer. 2.6 wt% Mn_3O_4-coated LNM exhibits excellent rate performance with the discharge capacity of 108 mAh/g, which is considerably higher than that of the uncoated LNM (78 mAh/g). The calculation of lithium ion diffusion coefficient in the materials illustrate that lithium diffusion is not hindered by the Mn_3O_4 coating layer. Meanwhile, the electrical conductivity of LNM (1.53×10^{-7} S/cm) is improved with 2.6 wt% Mn_3O_4 coating layer (3.15×10^{-5} S/cm), which may be because of the substantial content of Mn^{3+} ions on the surface. Moreover, 2.6 wt% Mn_3O_4-coated LNM shows good cycling stability with a capacity retention of 78% (*vs.* 67% for LNM) after 100 cycles at 55 °C.

Supplementary materials: FIG. S1 shows the XRD patterns of Mn_3O_4 formed by the manganese acetate alone at 400 °C for 5 h and in comparison with Mn_3O_4-PDF24-0734. The EIS measurements are also carried on the sintered pellets of the non-coated and 2.6% Mn_3O_4-coated LNM samples, as shown in FIG. S2. Table S1 is aimed to compare the surface modified LNM samples reported in literatures with this work.

V. ACKNOWLEDGEMENTS

This work was supported by the National Key R&D Program of China (No.2018YFB0905400), the Fundamental Research Funds for the Central Universities (No.JZ2019HGBZ0140), the National Natural Science Foundation of China (No.U1630106, No.51577175) and China Postdoctoral Science Foundation (No.172731). We are also grateful to Elementec Ltd. in Suzhou for the technical support.

[1] J. Lu, Y. L. Chang, B. H. Song, and H. Xia, J. Power Sources **271**, 604 (2014).
[2] J. Hassoun, S. Panero, P. Reale, and B. Scrosati, Adv. Mater. **21**, 4807 (2009).
[3] M. M. Deng, B. K. Zou, Y. Shao, and Z. F. Tang, J. Solid State Electrochem. **21**, 1733 (2017).
[4] B. Huang, X. Li, Z. Wang, and H. Guo, J. Alloys Compd. **583**, 313 (2014).
[5] X. L. Li, W. Guo, and Y. F. Liu, Electrochim. Acta **116**, 278 (2014).
[6] J. C. Arrebola, A. Caballero, L. Hernán, and J. Morales, J. Power Sources **195**, 4278 (2010).
[7] S. Tao, F. Kong, C. Wu, X. Su, and T. Xiang, J. Alloys Compd. **705**, 413 (2017).
[8] S. Niketic, M. Couillard, D. MacNeil, and Y. Abu-Lebdeh, J. Power Sources **271**, 285 (2014).
[9] H. Wang, Z. Shi, J. Li, and S. Yang, J. Power Sources **288**, 206 (2015).
[10] J. Chong, S. D. Xun, and J. P. Zhang, Chem. Eur. J. **20**, 7479 (2014).
[11] Y. R. Zhu, T. F. Yi, R. S. Zhu, and A. N. Zhou, Ceram. Int. **39**, 3087 (2013).
[12] F. Wu, N. Li, Y. Su, H. Lu, L. Zhang, R. An, Z. Wang, L. Bao, and S. Chen, J. Mater. Chem. **22**, 1489 (2012).
[13] S. Guo, H. Yu, P. Liu, X. Liu, D. Li, M. Chen, M. Ishida, and H. Zhou, J. Mater. Chem. A **2**, 4422 (2014).
[14] Y. Jin, Y. Xu, X. Sun, L. Xiong, and S. Mao, Appl. Surf. Sci. **384**, 125 (2016).
[15] M. M. Deng, Z. F. Tang, Y. Shao, X. D. He, Z. Y. Wen, and C. H. Chen, J. Alloys Compd. **762**, 163 (2018).
[16] Y. Y. Qian, Y. S. Fu, X. Wang, and H. Xia, J. Nanosci. Nanotechnol. **14**, 7038 (2014).
[17] R. Alcantara, M. Jaraba, and P. Lavela, Chem. Mater. **16**, 1573 (2004).
[18] M. Kunduraci, J. F. Al-Sharab, and G. G. Amatucci, Chem. Mater. **18**, 3585 (2006).
[19] Y. F. Deng, S. X. Zhao, Y. H. Xu, K. Gao, and C. W. Nan, Chem. Mater. **27**, 7734 (2015).
[20] T. Yang, N. Zhang, Y. Lang, and K. Sun, Electrochim. Acta **56**, 4058 (2011).
[21] B.K. Zou, H. Y. Wang, and Z. Y. Qiang, Electrochim. Acta **196**, 377 (2016).
[22] X. H. Rui, N. Ding, and J. Liu, Electrochim. Acta **55**, 2384 (2010).
[23] Q. T. Zhang, J. T. Mei, and X. M. Wang, Electrochim. Acta **143**, 265 (2014).
[24] X. W. Gao, Y. F. Deng, D. Wexler, G. H. Chen, S. L. Chou, H. K. Liu, Z. C. Shi, and J. Z. Wang, J. Mater. Chem. A **3**, 404 (2015).
[25] Z. Qiao, O. Sha, and Z. Y. Tang, Mater. Lett. **87**, 176 (2012).

DOI:10.1063/1674-0068/cjcp1906118

Articles

Improving the interfacial electrochemistry of $LiNi_{0.5}Mn_{1.5}O_4$ cathode by Mn_3O_4 coating

Miao-Miao Deng,[a,b] Da-Wei Zhang,[a] Yu Shao,[b] Xiao-Dong He,[b] Aqsa Yasmin,[b] Chun-Hua Chen*[b]

[a] *School of Chemistry and Chemical Engineering, Heifei University of Technology, Anhui Hefei 230009, China*

[b] *CAS Key Laboratory of Materials for Energy Conversions, Department of Materials Science and Engineering & Collaborative Innovation Center of Suzhou Nano Science and Technology, University of Science and Technology of China, Anhui Hefei 230026, China*

Abstract:

A Mn_3O_4 coating is approved to modify the surface of $LiNi_{0.5}Mn_{1.5}O_4$ particles by a simple wet grinding method for the first time, which realize an great improvement in electronic conductivity from $1.53 \cdot 10^{-7}$ S cm^{-1} to $3.15 \cdot 10^{-5}$ S cm^{-1} after 2.6% Mn_3O_4 coating. The electrochemical test resualts demonstrate that the Mn_3O_4 coating dramatically enhances both the rate performance and cycling capability (at 55 ℃) of $LiNi_{0.5}Mn_{1.5}O_4$. Among the samples, 2.6% Mn_3O_4-coated $LiNi_{0.5}Mn_{1.5}O_4$ not only exhibits excellent rate capability (a large capacity of 108 mAh g^{-1} at 10 C rate) but also

* Corresponding author. Tel.: +86 551 63606971; fax: +86-551-63601952. *E-mail address:*cchchen@ustc.edu.cn (Chun-Hua Chen)

keep 78% capacity retention at 55 ℃ and 1 C rate after 100 cycles.

摘要：

采用化学湿磨法，首次将金属氧化物 Mn_3O_4 包覆于 $LiNi_{0.5}Mn_{1.5}O_4$ 颗粒表面，使得电极材料的电子电导率从 $1.53 \cdot 10^{-7}$ S cm^{-1} 提高到 $3.15 \cdot 10^{-5}$ S cm^{-1}。电化学测试结果表明 Mn_3O_4 包覆大大提高 $LiNi_{0.5}Mn_{1.5}O_4$ 正极材料的倍率性能和高温循环稳定性。最佳包覆样品为 2.6 wt.% Mn_3O_4 包覆的 $LiNi_{0.5}Mn_{1.5}O_4$，在 10 C 倍率下具有 108 mA h g^{-1} 的高放电容并且在 55℃下 100 次循环后仍有 78%的容量保持率，远大于未包覆样品 67%的容量保持率。

Keywords: Lithium-ion batteries, cathode materials, spinel lithium nickel manganese oxide, surface modification, cathode-electrolyte interphase

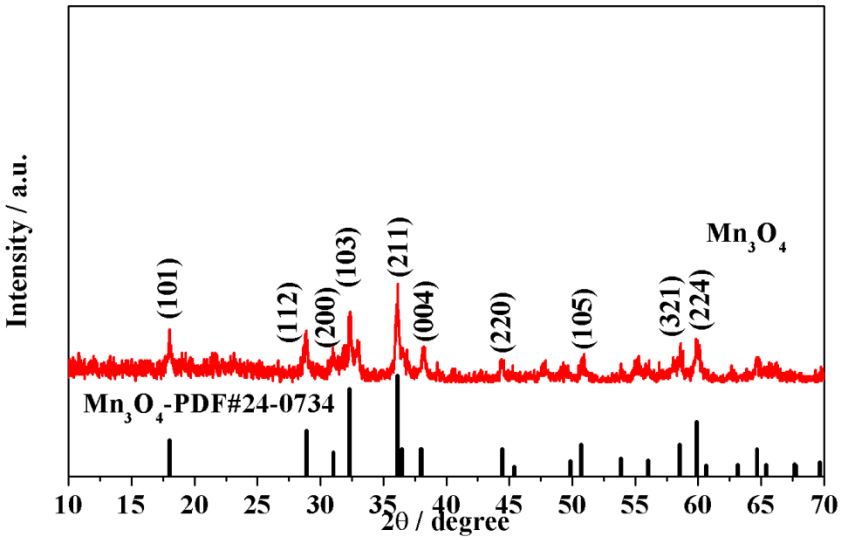

FIG. S1 XRD patterns of Mn_3O_4 formed by the manganese acetate alone at 400 ℃ for 5 h and Mn_3O_4-PDF#24-0734.

.

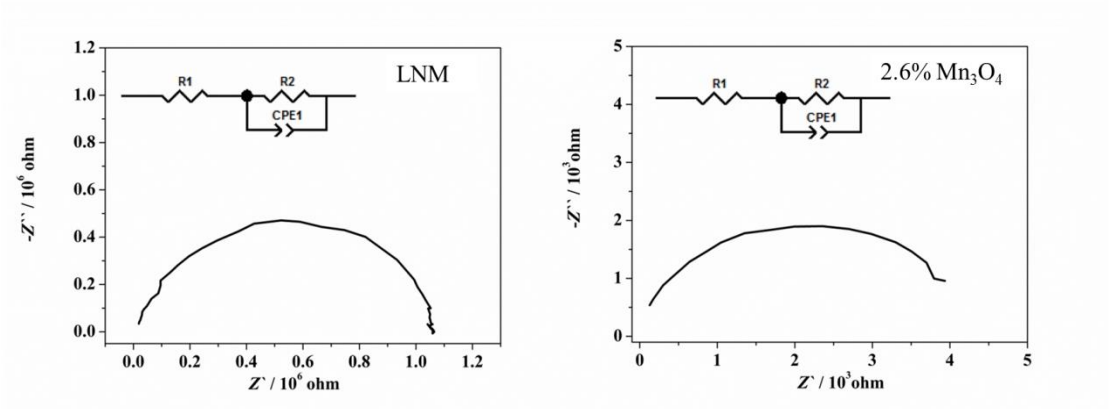

FIG. S2 EIS spectra for the sintered pellets: non-coated and 2.6% Mn_3O_4-coated LNM samples.

Table S1 Comparison of the electrochemical performance for surface modified LNM samples reported in literatures with this work.

Samples	Synthesis method	Rate performanc ($mAh\ g^{-1}$)	Capacity retention (%)	Reference
LNM/RuO_2	Precipitation	66.1@10C	97.7@0.5C, 100 cycles	[1]
LNM/C	Sol-gel	112@5C,104@10C	64.0@10C, 500 cycles	[9]
LNM/ZnO	Solution	–	87.5@2C, 50 cycles	[6]
LNM/CuO	Wet chemical	98.7@10C	95.0@0.5C, 100 cycles	[5]
LNM/Al_2O_3	Hydrothermal	–	76.6@0.5C, 300 cycles	[4]
LNM/TiO_2	Wet chemical	97.6@7C,88.3@10C	88.0@2C, 500 cycles	[7]
LNM/Li_3PO_4	Solid-state	–	93.3@0.5C, 300 cycles	[10]
LNM/PAALi	Wet chemical	111.4@6C,101.5@12C	90.0@0.2C, 200 cycles	[23]
LNM/$Li_4Ti_5O_{12}$	Sol-gel	–	100@0.2C, 100 cycles	[11]
LNM/PPy	Solution	105@2C,85@5C	95.0@1C , 300 cycles	[24]
LNM/($LiCoO_2$/Co_3O_4)	liquid-phase process	110@5C	99.4@1C , 100 cycles	[25]
LNM/Co_3O_4	Precipitation	116@6C, 97.5@10C	96.8@1C, 300 cycles	[15]
LNM/Mn_3O_4	Wet grinding	108@10C	115@1C, 200 cycles	This work